UNIVERSITI MALAYSIA PERLIS
UniMAP
International Journal of Nanoelectronics and Materials
IJNeaM
ISSN 1985-5761 | E-ISSN 2232-1535

The Hydrothermal Synthesis of TiO_2-GO with Enhance Photocatalytic Activity

Noor Azira Mohd Noor[a,*], Muhammad Asri Idris[a], Murizam Darus[b] and Nur Farhana Diyana Mohd Yunos[b]

[a]*Faculty of Chemical Engineering & Technology, Universiti Malaysia Perlis, Kompleks Pengajian Jejawi 2, Taman Muhibbah 02600 Arau, Perlis, Malaysia*
[b]*Faculty of Mechanical Engineering & Technology, Universiti Malaysia Perlis, Kampus Alam UniMAP, Pauh Putra, 02600 Arau, Perlis, Malaysia*
**Corresponding author. Tel.: +6049798154; fax: +6049798778; e-mail: noorazira@unimap.edu.my*

ABSTRACT

A composite material consisting of titanium dioxide and graphene oxide (TiO_2–GO) was synthesized through a hydrothermal reaction. This reaction involved the use of $Ti(SO_4)_2$ in an ethanol–water solvent. Different content of GO was studied to find the optimum parameter. The composites were subjected to characterization, encompassing an examination of their composition, structure, and microstructure through techniques such as X-ray diffraction (XRD), Raman spectra, scanning electron microscopy (SEM), and ultraviolet-visible diffuse reflectance spectroscopy. For Raman spectra, the presence of a G-band at approximately 1599 cm^{-1} and a D-band at 1350 cm^{-1} in the spectra indicates the presence of graphene oxide (GO). Therefore, the modified Hummer method synthesized graphite to GO. The findings for the XRD spectrum concerning the TiO_2–GO composites revealed the presence of finely dispersed anatase TiO_2 particles on the surface of the graphene oxide sheet layer. Diffraction pattern similar to pristine TiO_2, only for TiO_2–GO(0.75) and the peak for rutile TiO_2 at 2θ values 27.08° for both technique and TiO_2–GO(0.5) for spray technique. Apparently, GO sheets were almost covered by anchored TiO_2 particles, providing the possibility of efficient electronic conducting and electron transportation as in the SEM microstructures. EDS analysis shows the excessive carbon element for TiO_2-GO(0.75) and TiO_2-GO(1). The findings concerning the TiO_2–GO composites revealed the presence of finely dispersed anatase TiO_2 particles on the surface of the graphene oxide sheet layer. Notably, the photocatalytic performance of the TiO_2–GO composite significantly surpassed that of pure TiO_2 in the photodegradation of methyl blue (MB) when exposed to sunlight. The spray technique had a higher photocatalytic degradation percentage which is 82% for TiO_2-GO(0.25) compared to the dropped technique 79% which is TiO_2-GO(0.5). Degradation analysis of methyl blue concluded that the improved photocatalytic activity of TiO_2–GO primarily results from the enhanced efficiency in trapping and transporting electrons, which can be attributed to the presence of graphene oxide (GO).

Keywords: *TiO_2-GO composite, Graphene oxide, Hydrothermal method, Photocatalytic*

1. INTRODUCTION

During the past decades, photodegradation processes of organic pollutants as the best way for environmental remediation have attracted researchers and related industry attention [1,2]. Considering various oxide semiconductor photocatalysts, it indicates titanium dioxide (TiO_2) has properties that fulfill most design requirements including strong oxidation, long-term thermodynamic stability, cheapness, easy to fabricate and nontoxicity [3]. However, there are still certain drawbacks to consider, such as the reliance on ultraviolet (UV) light for activating photocatalysts, which greatly limits the technological practicality. Additionally, the low presence of UV light in the solar spectrum and its relatively poor absorption efficiency in sunlight are intriguing areas for exploration [1,2]. Furthermore, rapid recombination and photon scattering can negatively impact the efficiency of photocatalytic reactions involving the generation of electrons and holes in TiO_2 [4]. Therefore, it is essential to mitigate the recombination significantly of photoinduced electron-hole pairs and expand light absorption into the visible light region of the solar spectrum. These factors are crucial for enhancing the photocatalytic activity of TiO_2.

Researchers have addressed the challenges posed by the substantial band gap of TiO_2 (3.2 eV), as well as its sluggish reaction kinetics and rapid charge carrier recombination [4,5]. These problems can be solved by developing hybrid materials like TiO_2 photocatalysts that have a great visible light sensitivity, charge carrier separation capability and optimize the photocatalytic performance.

Graphene, a two-dimensional (2D) carbon material bonded with sp^2 hybridization, has garnered significant attention since 2004 due to its exceptional thermal, mechanical, cost-effectiveness, electrical, and optical properties [4,5]. One effective approach to creating composite materials and enhancing the characteristics of TiO_2, while harnessing the distinctive attributes of graphene, involves depositing additional materials onto graphene sheets. Previous studies have shown that composites of TiO_2 with various carbon-based materials, such as carbon nanotubes, activated carbon, and fullerenes, exhibit improved photocatalytic performance compared to pure TiO_2 [6].

Hence, it is of great interest to explore the substantial impact of the graphene oxide (GO) content on photocatalysis. Graphene oxide is a material derived from graphene, which is known for its unique properties, including excellent electrical conductivity and a large surface area. It is interesting exploring how incorporating graphene oxide into photocatalytic materials can enhance their performance. The hydrothermal method is chosen to synthesize the TiO_2-GO composite. This step is crucial because the properties of GO, such as its structure and size, can influence how it interacts with other materials like titanium dioxide (TiO_2) in the subsequent steps. In this study, we focus on the synthesis of GO and the creation of TiO_2-GO composites, varying the GO-to-TiO_2 ratio and employing two distinct fabrication techniques for these composites. In the first method, the resulting products were dropped onto square silica substrates. This technique involves physically depositing the composite material onto a solid surface, possibly allowing for precise control over the coating thickness and distribution. Meanwhile the second method involved using a spray technique onto the square silica substrates to coat square silica substrates with the TiO_2-GO composites. This technique likely allows for a more uniform and thin coating by atomizing the composite mixture and evenly distributing it onto the substrate.

Overall, this research study is focused on examining how the GO content, preparation methods, and composite ratios affect the photocatalytic properties of TiO_2-GO composites. The findings from this study could have implications for the development of more efficient and effective photocatalytic materials with potential applications in various fields, such as environmental remediation and renewable energy generation.

2. MATERIALS AND METHODS

The synthesis of TiO_2-GO composites involved a hydrothermal reaction, while the production of graphene oxide (GO) was achieved by utilizing graphite powder as a precursor and employing the modified Hummers method.

2.1. Synthesis of GO

The initial step of the synthesis process commenced with the oxidation of graphite. To achieve this, a mixture containing sulfuric acid (H_2SO_4:H_3PO_4 in a ratio of 180:20 ml), graphite powder (1.5 g), and potassium permanganate ($KMnO_4$, 9.0 g) was prepared. This mixture was subjected to continuous stirring using a magnetic stirrer at a consistent speed for 6 hours. Subsequently, the mixture was poured into approximately 200 ml of ice water, and hydrogen peroxide (H_2O_2) was added to terminate the oxidation process. The resulting solution was then subjected to centrifugation for 7 minutes to obtain graphene oxide (GO). Afterward, hydrochloric acid (HCl) was employed to decant and remove the supernatant. The washing process was repeated multiple times.

2.2. Synthesis of TiO_2-GO

To produce the TiO_2-GO composites, we utilized titanium (IV) sulfate ($Ti(SO_4)_2$) and a GO aqueous suspension as our starting materials. The process commenced by adding 0.12 ml of $Ti(SO_4)_2$ into 5 ml of ethanol, and then a specific quantity of GO suspension was gradually introduced. The ratio amount of $Ti(SO_4)_2$ to GO suspension are 1:0.1, 1:0.251:0.5, 1:075, and 1:1 known as TiO_2-GO(0.01), TiO_2-GO(0.25), TiO_2-GO(0.5), TiO_2-GO(0.75) and TiO_2-GO(1).

Reference samples were fabricated without additional GO suspension known as TiO_2. Afterwards, deionized (DI) water was gradually introduced into the beaker until the total volume reached 10 ml. The mixture was consistently stirred, and the resulting solution was then transferred into a 5 ml Teflon-sealed autoclave. It was subjected to soaking at 180 °C in a furnace for a duration of 9 hours. Subsequently, the obtained products were separated through centrifugation and underwent multiple washes with both deionized water and ethanol. Following this purification process, the resulting products were either deposited onto silica substrates in the first method or utilized in the fabrication of the composites via the spray method in the second approach. The TiO_2-GO d for 12 h in an oven at 70 °C.

2.3. Characterizations

Raman spectroscopy analysis was employed to confirm the transformation of graphite into graphene oxide using the modified Hummers method. The Raman spectra were acquired using a Renishaw Raman Microscope (WITEC, Germany). To investigate the crystal structures of the carbonaceous materials, X-ray diffraction (XRD) analysis was conducted at various stages of synthesis. This characterization was performed on a Bruker D8 diffractometer, utilizing Cu Ka radiation (λ = 1.5406 Å) at 40 kV and 40 mA.

Microstructure analysis was carried out using scanning electron microscopy (SEM) imaging, and energy-dispersive X-ray spectroscopy (EDS) analysis was performed using a Hitachi S-4800 field emission scanning electron microscope.

2.4. Photocatalytic Activity Measurement

In this experiment, the TiO_2-GO composites were immersed in an aqueous solution of methyl blue (MB). In the context of methyl blue (MB) photodegradation, samples were systematically collected at 30-minute intervals. The absorbance of MB concentration in all the samples after photodegradation was measured at the maximum peak of 665 nm using visible spectrophotometer Genesys 20.

3. RESULTS AND DISCUSSION

Raman spectroscopy was employed to analyze carbonaceous materials whether it is in the ordered or disordered crystal structures. Figure 1 displays the Raman spectra for both carbonaceous materials, used as the precursor, and graphene synthesized through the modified Hummers method. In the spectra, three distinct Raman-active bands are clearly observed. These include the G band, which represents the in-phase vibration of the graphite lattice, as well as the relatively weaker disorder band at 1551 cm^{-1} attributed to the edges of the graphite structure, known as the D band at 1330 cm^{-1}. Additionally, a peak at 2655 cm^{-1} is also found.

The presence of a G-band at approximately 1599 cm^{-1} and a D-band at 1350 cm^{-1} in the spectra indicates the presence of graphene oxide (GO). This observation aligns with findings from previous studies by Chen et al. and Oppong et al. [6,7]. In these spectra, the G-band is associated with graphitic carbon, while the D-band signifies structural defects or partially disordered graphitic domains [8]. Notably, the strong D-bands in both spectra indicate lattice distortions in the graphene basal planes. It's worth noting that Raman-inactive regions remain so until the edges, causing a "lighting up" effect due to symmetry breaking and changes in the selection rules for lattice vibrations, resulting in the appearance of the D-band at a specific frequency on the infinite graphene sheet. Furthermore, the higher degree of disorder in graphite contributes to a broader G-band and a broader D-band with a higher relative intensity compared to the G-band. In fact, as amorphous carbon contains a certain proportion of sp^3 carbons, both the G and D-bands undergo changes when graphite becomes amorphous.

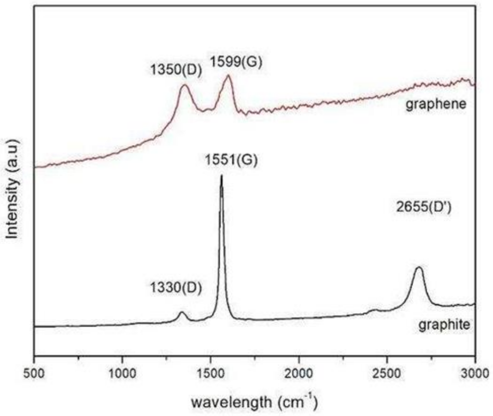

Figure 1. Raman spectrum for graphite and graphene after synthesis.

The XRD patterns displayed in Figure 2 reveal the characteristic features of both graphite and graphene oxide (GO) synthesized using the modified Hummers method. In the case of graphite, a distinctive peak is observed at 2θ = 27°. On the other hand, the XRD pattern for GO exhibits a peak at 2θ = 10.75°. This specific peak in GO corresponds to the [111] space group and signifies a cubic crystal structure. As per the findings reported by N.I. Zaaba et al. [9], when graphite undergoes oxidation and transforms into GO, a notable shift in the XRD peak occurs, moving from around 26° for graphite to approximately 11° for GO. Therefore, the XRD data provided here strongly support the conclusion that the modified Hummers method successfully converted graphite into GO, as evident in Figure 2.

Figure 3 showed the XRD characterization of TiO$_2$-GO composites synthesis under hydrothermal method at different ratio amount GO for both fabrication route which are dropped and spray technique. The TiO$_2$-GO composite clearly reveals the presence of distinctive diffraction peaks characteristic of anisotropic anatase TiO$_2$. However, the orderly stacking of GO has been disrupted because of the intercalation of TiO$_2$, leading to the absence of the typical GO peak in the TiO$_2$-GO composites [10].

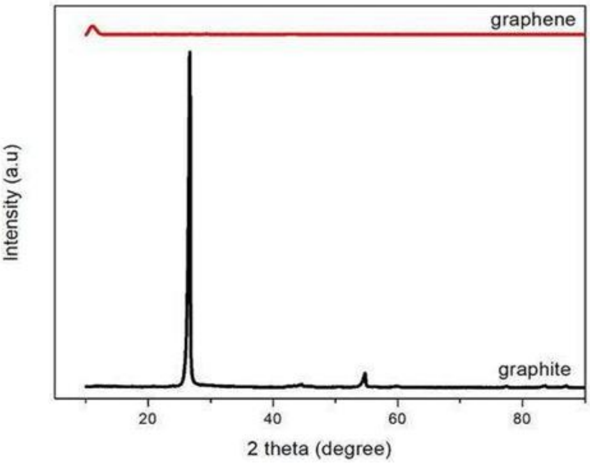

Figure 2. XRD spectrum for graphite and graphene.

The characteristic peaks observed for reference sample TiO$_2$ at 2θ values 25.63°, 33.5°, 47.6° and 53° corresponding to the (101), (110), (200) and (105) crystallographic planes of anatase TiO$_2$ respectively (ICDD 01-089-4203). The diffraction pattern is similar to pristine TiO$_2$, only for TiO$_2$–GO(0.75) and the peak for rutile TiO$_2$ at 2θ values 27.08° for both techniques and TiO$_2$–GO(0.5) for spray technique. The absence of a distinct diffraction peak associated with GO's characteristic pattern can be attributed to the uniform growth of TiO$_2$ particles on the graphene sheet, which occurs due to the exfoliation of the GO sheet. It also prevents recurrent restacking [11]. TiO$_2$-GO composite is broader when compared to the peaks of bare TiO$_2$. This is because the distortion of the lattice structure of TiO$_2$ made the interaction with the GO. Therefore, the crystalline structure of TiO$_2$ on GO does not appear strongly. Meanwhile, peak broadening shows a decrease in particle size. Using the Scherrer equation, the calculated crystallite sizes for the composites, based on the (101) peak, have fallen within the range of 4–5 nm. These sizes were notably smaller than those of bare TiO$_2$, which were approximately 11 nm [12]. Peak at 15° and 21.9° indicates the presence of silicon resulting from the substrate.

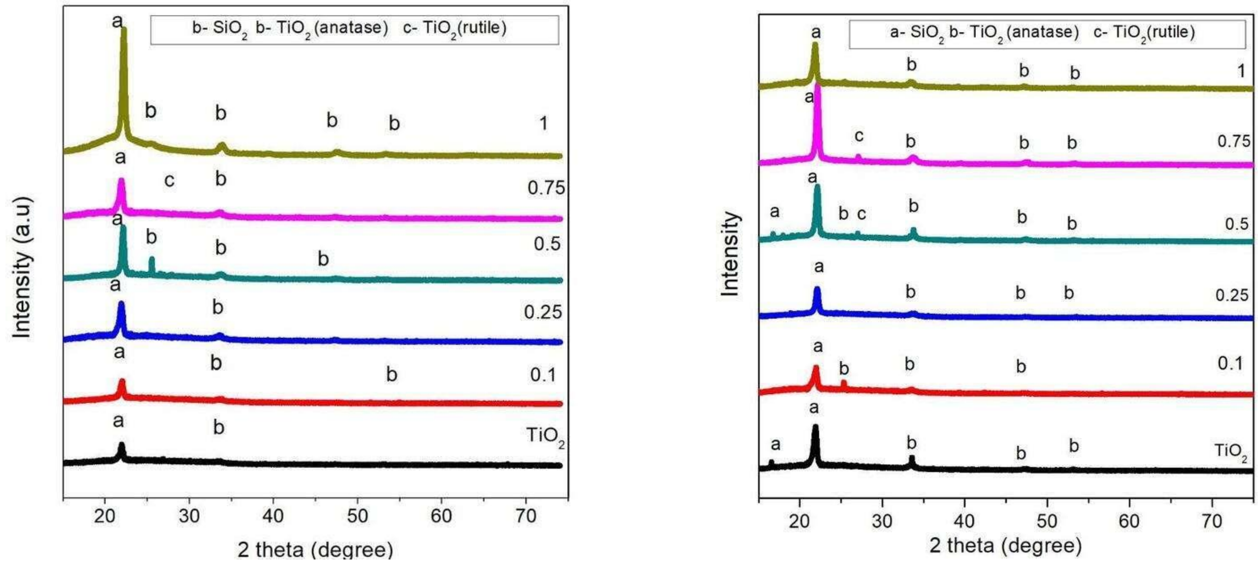

(a)

(b)

Figure 3. The XRD spectrum of TiO_2-GO composites synthesis under hydrothermal method at different ratios of TiO_2 to GO suspension for both fabrication routes, (a) dropped and (b) spray technique.

The SEM image in Figure 4 reveals noticeable distinctions in the morphology between graphite and graphene oxide. It is evident that in the case of graphite, the sheets are closely stacked together. In contrast, for graphene oxide, the sheets appear to be exfoliated, with a more separated and dispersed structure. This exfoliation of graphite into graphene oxide is consistent with findings reported by Paulchamy et al. [13].

Prior to the microstructure shown in Figure 5, many platelets of TiO_2-GO composites uniformly stacking in between large aggregates of TiO_2 particles showed increased adsorption compared to TiO_2. Consequently, it can be inferred that the surface area of the composite material surpasses that of bare TiO_2. This increase in surface area is particularly evident when comparing the higher GO ratios, ranging from TiO_2-GO(0.01) to TiO_2-GO(1), with bare TiO_2, especially when using the drop technique. Additionally, the homogenous and uniform distribution of TiO_2 particles on each individual GO sheet, along with their accumulation along the wrinkles of the GO, is visibly prominent in the case of TiO_2-GO(0.01), TiO_2-GO(0.25), and TiO_2-GO(0.5). The excessive GO sheet can be seen in TiO_2-GO (0.75) and TiO_2-GO(1).

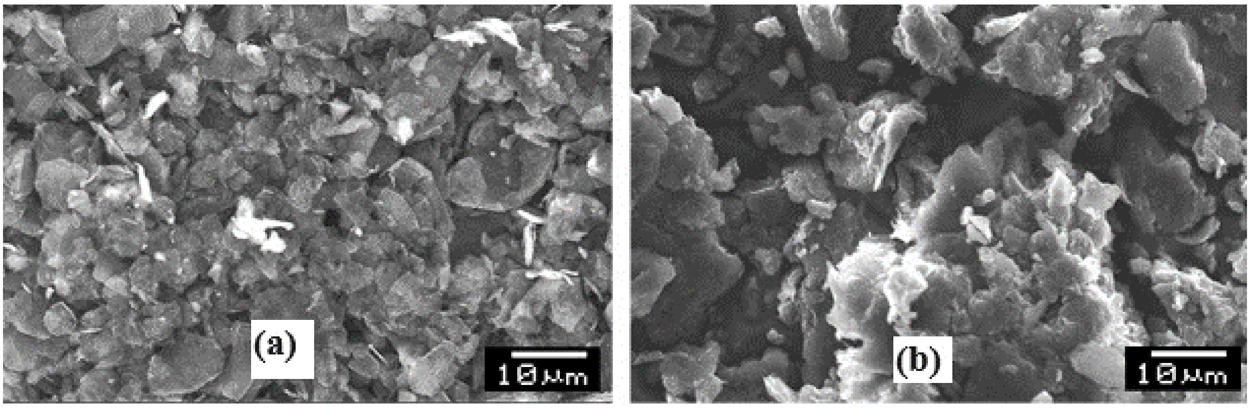

Figure 4. SEM morphology at 1000x magnification for (a) graphite and (b) GO.

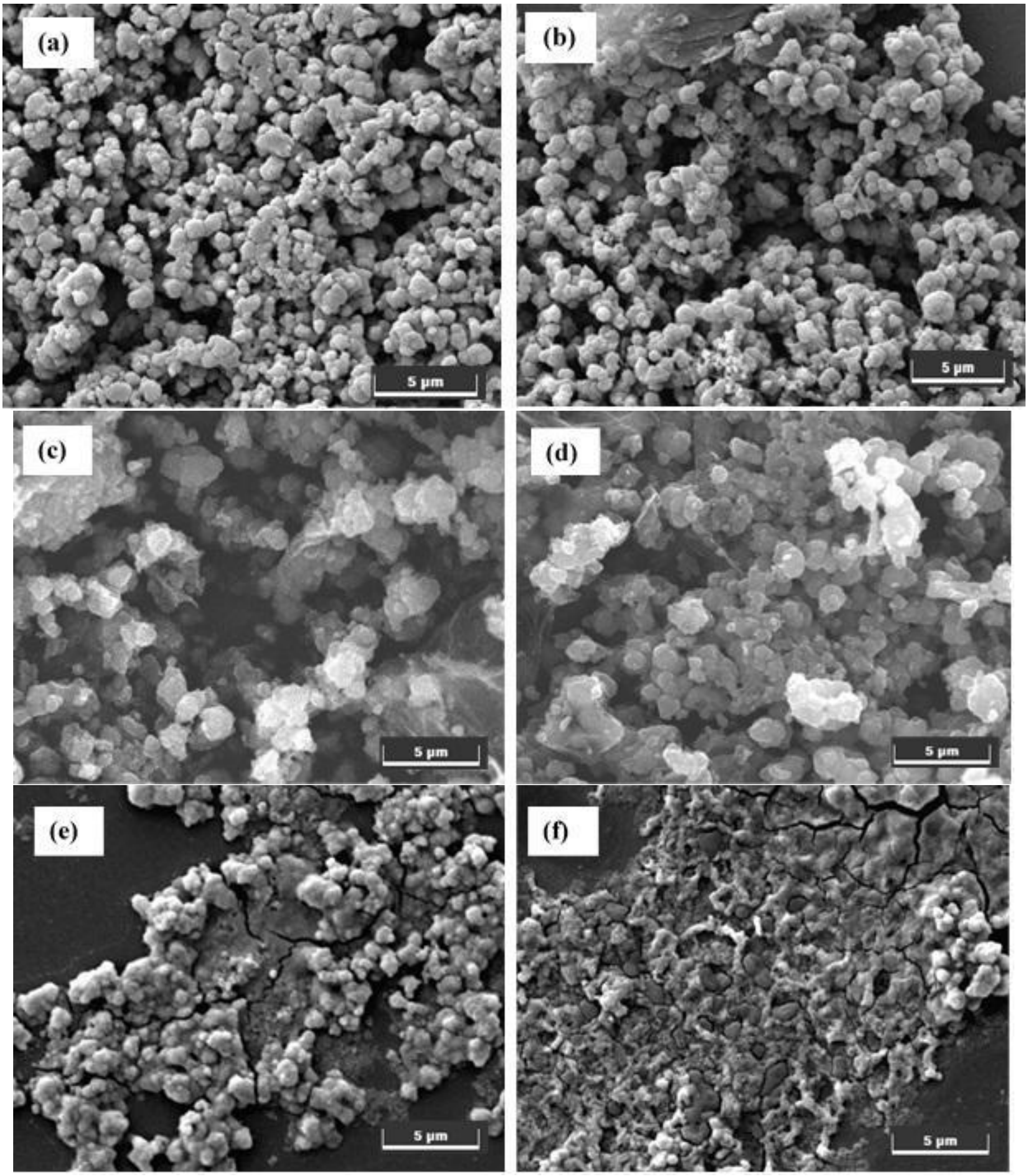

Figure 5. SEM morphology at 5000x magnification for the reference sample, TiO_2, TiO_2-GO composites synthesis using dropped technique at different ratio amount of TiO_2 to GO suspension are (a) TiO_2, (b) TiO_2-GO(0.01), (c) TiO_2-GO(0.25), (d) TiO_2-GO(0.5), (e) TiO_2-GO(0.75) and (f) TiO_2-GO(1) respectively.

The EDS of the microstructure shown in Figure 6 is for TiO_2-GO(0.01) using dropped technique show P1 is the GO sheet and P2 is TiO_2. For P1 the atomic % and weight % is 100% element carbon, therefore it clearly shows the GO sheet. For P2 the atomic % for oxygen is 70.91% and titanium is 29.09%. For the weight %, oxygen is 44.9% and titanium 55.10. Figure 7 shows EDS analysis for TiO_2-G (1) using dropped technique, the P3 is the stacking of GO and TiO_2, the element analysis indicated that the weight% for carbon is 9.82%, titanium is 10.08% and the rest is oxygen 80.10%. Besides, for the atomic% its show the excessive carbon element which are 13.55% for carbon, titanium 3.49% and oxygen is 82.96%.

Figure 8 shows the microstructure for the spray technique, large aggregated TiO_2 particles were seen in between the TiO_2-GO platelets. Indeed, it's worth noting that graphene oxide (GO) typically consists of multiple sheets and retains a layered structure, which is accompanied by micrometer-long wrinkles. During hydrothermal synthesis, there was self-assembly of the TiO_2 on the GO sheet. It contributes to the well distribution of TiO_2 on both sides of the GO sheet [14]. Figure 9 shows EDS analysis for TiO_2-G (0.25) using spray technique, the P4 is the stacking of GO and TiO_2, the element analysis indicated that the weight% for carbon is 13.26%, titanium is 51.95% and the rest is oxygen 34.79%. Besides, for the atomic% it shows the excessive carbon element which is 25.30% for carbon, titanium 24.87% and oxygen is 49.83%. Apparently, GO sheets were almost covered by anchored TiO_2 particles, providing the possibility of efficient electronic conducting and electron transportation [15].

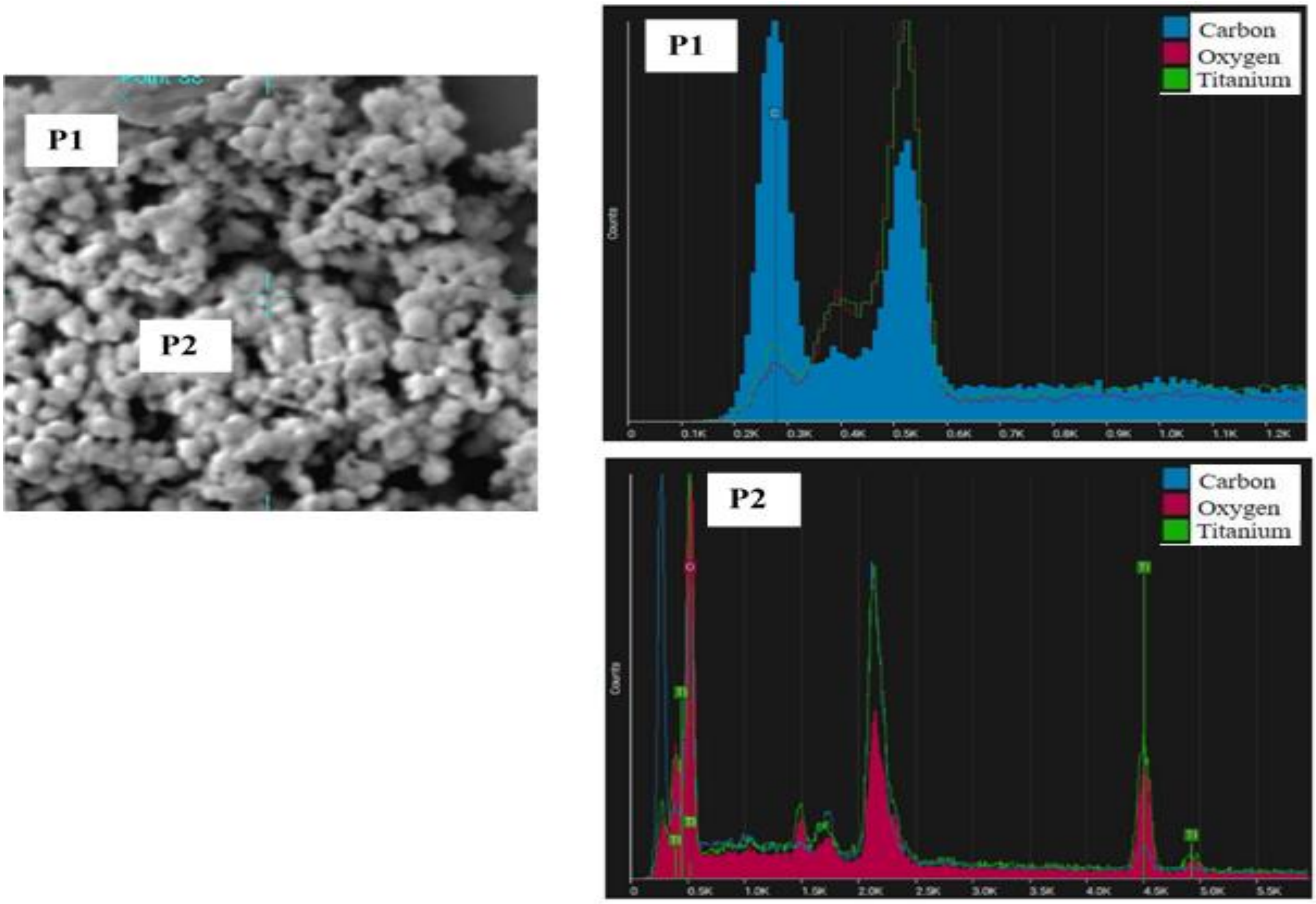

Figure 6. EDS analysis for TiO_2-GO(0.01) using dropped technique show P1 is the GO sheet and P2 is TiO_2.

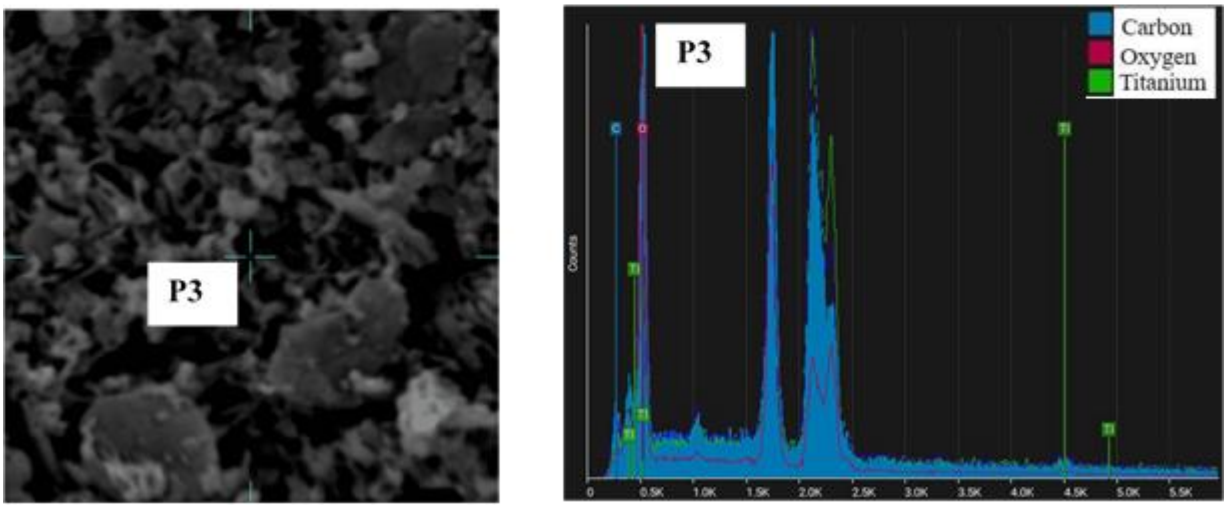

Figure 7. EDS analysis for TiO_2-GO(1) using dropped technique show P3 is consist of carbon, titanium and oxygen.

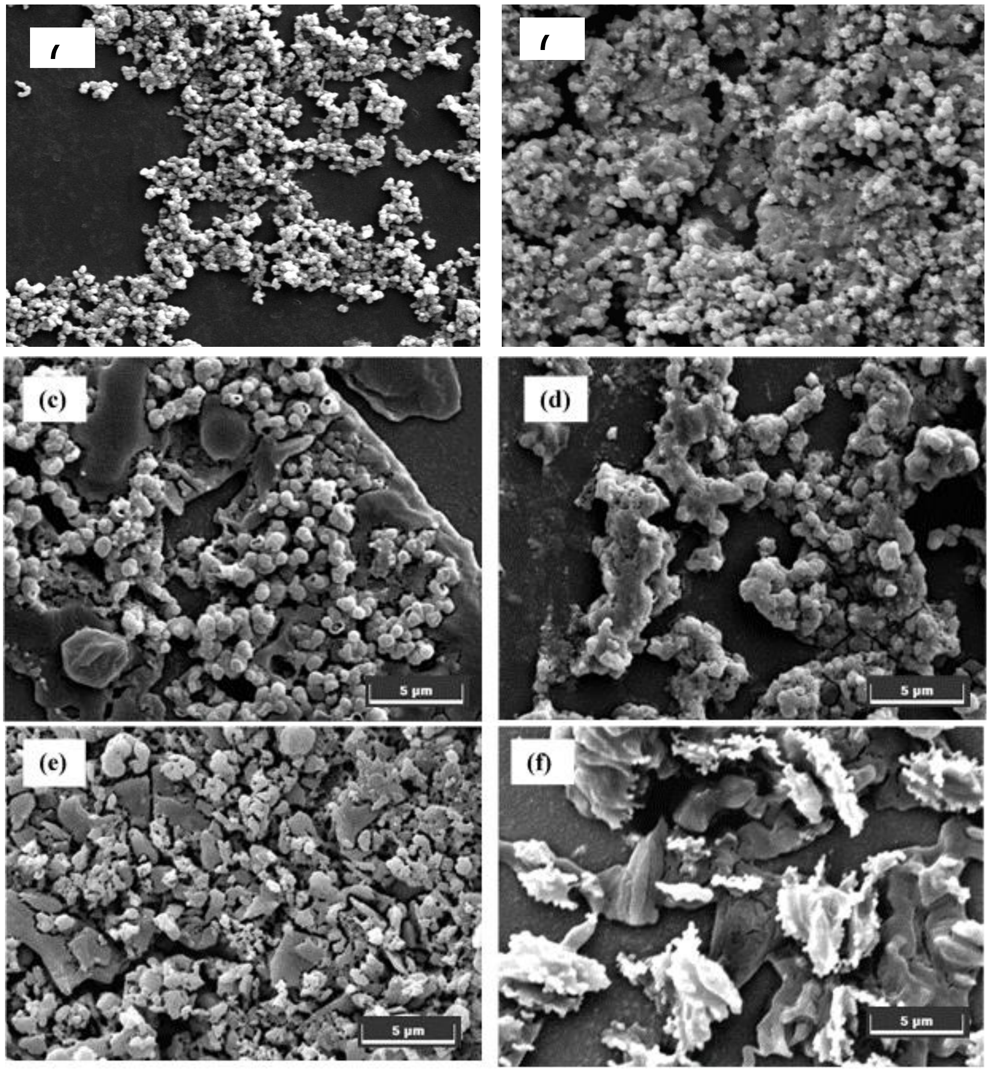

Figure 8. The SEM morphology at 5000x magnification for the reference sample, TiO_2, TiO_2-GO composites synthesis using spray technique at different ratio amount of TiO_2 to GO suspension are (a) TiO_2, (b) TiO_2-GO(0.01), (c) TiO_2-GO(0.25), (d) TiO_2-GO(0.5), (e) TiO_2-GO(0.75) and (f) TiO_2-GO(1) respectively.

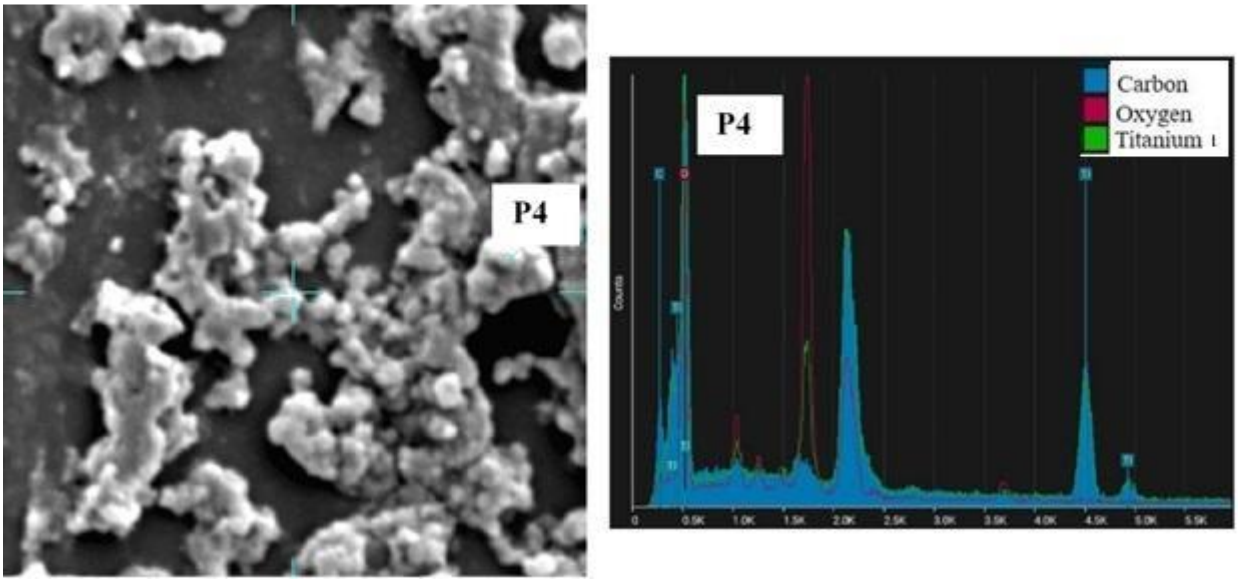

Figure 9. EDS analysis for TiO_2-GO (0.25) using spray technique shows P4 is consist of carbon, titanium and oxygen.

Confirmation of the homogeneous self-assembly of TiO_2 onto GO Sheets on a silica substrate via hydrothermal synthesis validated by Raman spectra, XRD spectra, SEM, and EDS analysis is consistent with the findings of Liu et al. In their study, GO and Degussa P25 were employed to create GO-P25 composites because P25 had limited dispersion in deionized water; only a portion of the P25 nanoparticles adhered to the GO sheet. Hydrothermal synthesis offered ease of control, such as adjusting the GO-to-TiO_2 ratio.

Hydrothermal method for TiO_2-GO composite at all loading of RGO is more active than the bare TiO_2 synthesized [12]. Figure 10 showed the progression of photocatalytic degradation over time, as measured against irradiation duration under sunlight for the TiO_2-GO composite. The photocatalytic degradation displayed a consistent increase with the passage of time. According to the result obtained, 60 minutes before the photocatalytic takes place where samples were in the dark, it was shown that the absorption of MB onto the surface of the composite is about the same for all samples, around 2 to 15% as can be seen in Table 1. Following a 60-minute exposure, the samples were subjected to sunlight for photocatalytic evaluation. The percentage of MB degradation under sunlight irradiation exhibited an upward trend as the amount of GO increased.

However, the degradation percentage began to decrease after reaching a peak at TiO_2-GO(0.5) when employing the dropped technique. Meanwhile, the spray technique increases at TiO_2-GO(0.25) and slowly decreases with the increment of GO. Therefore, the optimum photocatalytic activity is TiO_2-GO(0.5) for dropped technique and TiO_2-GO(0.25) for the spray technique. The spray technique had a higher photocatalytic degradation percentage which is 82% for TiO_2-GO(0.25) compared to dropped technique 79% which is TiO_2-GO(0.5). It is because the TiO_2 particle can disperse well and stack in between the GO sheet.
Methylene blue (MB) molecules initially adhered to the surface of the GO sheet, and subsequently, the photocarriers on the TiO_2 participated in the photodegradation process. Zhang and Pan's research highlighted the role of GO as a catalyst carrier, effectively expediting the rate of photocatalytic reactions [16]. It has been established that GO enhances the photocatalytic performance of TiO_2 through a synergistic effect, as well as the establishment of π-π conjugation between MB molecules (or other pollutants) and aromatic rings. Additionally, it helps in delaying charge recombination under UV light exposure.

However, it is worth noting that in the experiments conducted, no degradation of methylene blue was observed over an extended period. This lack of degradation can be attributed to the low crystallinity of the materials involved and the presence of residual surfactant impurities within their respective pore walls [17].

Prior to the graph shown in Figure 10, when compared to the bare TiO_2 used as a reference sample, the TiO_2-GO composite exhibited enhanced adsorption characteristics. This improvement can be attributed to the increased surface area resulting from the layered composite formation. The presence of GO sheets, known for their efficient electron trapping and transport properties, effectively curbs the recombination of photogenerated electron-hole pairs in TiO_2. Furthermore, the composite structures featuring well-formed anatase crystal TiO_2 with small crystallite sizes, close interfacial contact, and a narrow band gap contribute to enhanced light absorption and efficient electron transport. These combined factors ultimately lead to an improvement in the photocatalytic performance of TiO_2-GO.

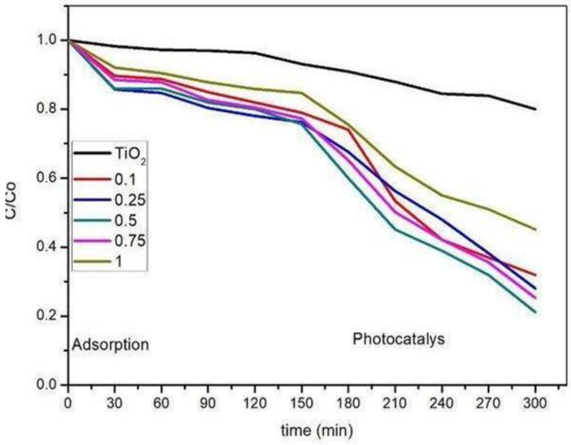

(a)

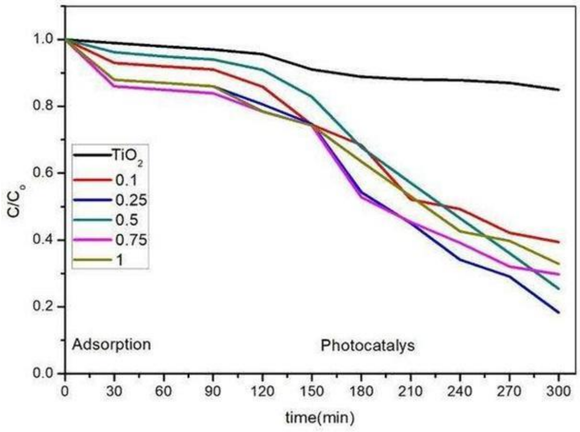

(b)

Figure 10. Photodegradation of TiO_2-GO composites synthesis under hydrothermal method at different ratio amount of TiO_2 to GO suspension are TiO_2-GO(0.01), TiO_2-GO(0.25), TiO_2-GO(0.5), TiO_2-GO(0.75) and TiO_2-GO(1). The technique for fabrication of the composite using (a) Dropped and (b) Spray technique.

Table 1 The rate of photocatalytic degradation

Samples	%MB absorbance in the dark (%)		%MB degradation under sunlight irradiation (%)	
	Dropped	Spray	Dropped	Spray
TiO_2	3	2	20	15
TiO_2-GO(0.01)	11	8	68	61
TiO_2-GO(0.25)	15	13	72	82
TiO_2-GO(0.5)	14	14	79	75
TiO_2-GO(0.75)	12	15	75	71
TiO_2-GO(1)	10	13	55	67

Graphene oxide (GO) serves multiple roles in the photocatalytic process, acting as an adsorbent, electron acceptor, and photosensitizer, which collectively enhance the photodecomposition process with greater efficiency. Similarly, titanium nanotubes (TNT) exhibit a comparable structure to that of the GO sheet and are responsible for electron transport across the sheet's surface. This electron transport process leads to a reaction with adsorbed oxygen (O_2), resulting in the formation of hydroxyl radicals (·OH), a crucial step in the photocatalytic degradation of methylene blue (MB). Carbonaceous materials are said to have exceptional and excellent adsorption properties and are widely used in various applications in protecting the environment. As reported by Wang et al. most industrial using dyes and pollutants released into rivers are aromatic and expertise interested in creating stacking and layer interactions with the aromatic domains of graphene is appropriate [17].

4. CONCLUSION

In conclusion, one step method hydrothermal could grow TiO_2 on GO using different techniques to fabricate the composite which is dropped and spray technique. Both techniques produced a TiO_2-GO composite with strong interactions between TiO_2 and GO sheet. The resultant composite material demonstrates outstanding photocatalytic activity when compared to pure TiO_2 combined with various other diverse materials. But the different ratio of GO gives some effect to the photocatalytic. The best ratio for dropped technique is TiO_2-GO (0.5) and for spray technique is TiO_2-GO (0.25). Significant enhancement corresponded to the synergistic effect between TiO_2 particles and GO sheets makes it suitable for photocatalytic activity. Meanwhile, the TiO_2 particle can disperse well and stack in between the GO sheet for spray technique. Therefore, the small amount of GO can contribute to the optimum properties for TiO2-GO composite,

ACKNOWLEDGMENTS

The research was supported by the Fundamental Research Grant Scheme, FRGS 2021: 9003-00919 (FRGS/1/2021/STG05/UNIMAP/02/6). The authors would like to acknowledge Faculty of Chemical Engineering & Technology, Management & Innovation Centre (RMIC) of Universiti Malaysia Perlis.

REFERENCES

[1] C. Byrne, G. Subramanian, S. C. Pillai. (2018), Recent advances in photocatalysis for environment applications, Journal of Environmental Chemical Engineering. Vol. 6, Issue 3, 3531-3555.

[2] M. Najafi, A. Kermanpur, M. R. Rahimipour, A. Najafizadeh (2017). Effect of TiO_2 morphology on structure of TiO_2-graphene oxide nanocomposite synthesized via a one-step hydrothermal method, Journal of Alloys and Compounds. Vol. 722, 272–277.

[3] Yan Liu (2014). Hydrothermal synthesis of TiO_2–RGO composites and their improved photocatalytic activity in visible light, RSC Advances. Vol. 4, 36040-36045.

[4] D. A. C. Brownson, D. K. Kampouris and C. E. Banks (2011). An overview of graphene in energy production and storage applications. Journal of Power Sources. Vol. 11, 4873–4885.

[5] H. Zhang, X. Lv, Y. Li, Y. Wang, J. Li (2010). P25-Graphene Composite as a High Performance Photocatalyst, ACS Nano. Vol. 4, Issue 1, 380–386.

[6] M. Sohail, H. Xue, Q. Jiao, H, Li, K. Khan, S. Wang, Y. Zhao (2017). Synthesis of well-dispersed TiO_2@reduced graphene oxide (rGO) nanocomposites and their photocatalytic properties, Materials Research Bulletin. Vol. 90, 125–130.

[7] Ji Chen, Bowen Yao, Chun Li, Gaoquan Shi (2013). An improved Hummers method for eco- friendly synthesis of graphene oxide synthesis of graphene oxidevol, Carbon. Vol. 64, 225–229.

[8] Oppong, S. O., Opuka, F., Golender, P. P. (2019) Tuning the electronic and structural properties of Gd-TiO2-GO nanocomposites for enhancing photodegradation of IC dye: The role of Gd3+ ion, Applied Catalysis B: Enviromental. Vol. 243, 106-120.

[9] K. N. Kudin, B. Ozbas, H. C. Schniepp, R. K. Prud'homme, I. A. Aksay, R. Car, (2008). Raman spectra of graphite oxide and functionalized graphene sheets. Nano Letters. Vol. 8, Issue 1, 36–41.

[10] N. I. Zaaba, K. L. Foo, U. Hashim, S. J. Tan, Wei-Wen Liu, C. H. Voon. (2017). Synthesis of Graphene Oxide using Modified Hummers Method: Solvent Influence, Procedia Engineering. Vol. 184, 469-477

[11] J. Liu, H. Bai, Y. Wang, Z. Liu, X. Zhang, D. D. Sun, (2010). Self-Assembling TiO_2 Nanorods on Large Graphene Oxide Sheets at a Two-Phase Interface and Their Anti-Recombination in Photocatalytic Applications, Advanced Functional Materials., Vol. 20, Issue 23, 4175–4181.

[12] Kavitha MK, Pillai SC, Gopinath P, John H (2015). Hydrothermal synthesis of ZnO decorated reduced graphene oxide: understanding the mechanism of photocatalysis. J Environ Chem Eng. Vol. 3, Issue 2,1194–1199.

[13] Deepthi John, A. S. Rajalakshmi, Raichel Mary Lopez, V. Sivanandan Achari (2020). TiO_2-reduced graphene oxide nanocomposites for the trace removal of diclofenac, SN Applied Sciences. Vol. 2.

[14] B. Paulchamy, G. Arthi, B. D. Lignesh, J. (2015). A Simple Approach to Stepwise Synthesis of Graphene Oxide Nanomaterial, Nanomed Nanotechnol. Vol. 6, Issue 1, 2–5.

[15] Sanjaya D. Perera, Ruperto G. Mariano, Khiem Vu, Nijem Nour, Olive Seitz, Yves Chabal and Kenneth J. Balkus, Jr (2012). Hydrothermal synthesis of graphene-TiO2nanotube composites with enhanced photocatalytic activity, ACS Catalysis. Vol. 2, Issue 6, 949-956.

[16] Yuyu Ren, Lili Zhoa, Yang Zou, Lixin Song, Ningning Dong, Jun Wang (2019). Effects of Different TiO2 Particle Sizes on the Microstructure and Optical Limiting Properties of TiO_2/Reduced Graphene Oxide, Nanocomposites. Vol. 9, Issue 5, 1-16

[17] Q. Zhang, Y. Q. He, X. Chen, D. Hu, L. J. Li, T. Yin, L. L. Ji, (2011). Structure and photocatalytic properties of TiO2-Graphene Oxide intercalated composite, Chinese Science Bulletin. Vol. 56, Issue 3, 331–339.

[18] G. Wang, L. Xu, J. Zhang. T. Yin, D. Han, (2012). Enhanced Photocatalytic Activity of Powders (P25) via Calcination Treatment, International Journal of Photoenergy.